Journal of Geophysical Research: Oceans

RESEARCH ARTICLE
10.1029/2018JC014195

Key Points:
- WFS surface water shows a change from carbon sink to source from 1996 to 2016
- The WFS emits 9.23 Tg C/year, with the south nearshore emitting the most at 9.01 Tg C/year and the north acting as a sink of −1.96 Tg C/year
- Shelf water (<40-m isobath) pCO_2 has increased at a rate approximately 2.6 times faster than the atmospheric rate in the past 20 years

Supporting Information:
- Supporting Information S1

Correspondence to:
L. L. Robbins,
llrobbins@mail.usf.edu

Citation:
Robbins, L. L., Daly, K. L., Barbero, L., Wanninkhof, R., He, R., Zong, H., et al. (2018). Spatial and temporal variability of pCO_2, carbon fluxes, and saturation state on the West Florida Shelf. *Journal of Geophysical Research: Oceans*, *123*, 6174–6188. https://doi.org/10.1029/2018JC014195

Received 25 MAY 2018
Accepted 7 AUG 2018
Accepted article online 20 AUG 2018
Published online 3 SEP 2018

Spatial and Temporal Variability of pCO_2, Carbon Fluxes, and Saturation State on the West Florida Shelf

L. L. Robbins[1], K. L. Daly[1], L. Barbero[2,3], R. Wanninkhof[3], R. He[4], H. Zong[4], J. T. Lisle[5], W.-J. Cai[6], and C. G. Smith[5]

[1]College of Marine Science, University of South Florida, Tampa, FL, USA, [2]Cooperative Institute for Marine and Atmospheric Studies, University of Miami, Coral Gables, FL, USA, [3]NOAA's Atlantic Oceanographic and Meteorological Laboratory, Miami, FL, USA, [4]Marine Earth and Atmospheric Sciences, North Carolina State University at Raleigh, Raleigh, NC, USA, [5]U.S. Geological Survey, St. Petersburg, FL, USA, [6]School of Marine Science and Policy, University of Delaware, Newark, DE, USA

Abstract The West Florida Shelf (WFS) is a source of uncertainty for the Gulf of Mexico carbon budget. Data from the synthesis of approximately 135,000 pCO_2 values from 97 cruises from the WFS show that the shelf waters fluctuate between being a weak source to a weak sink of carbon. Overall, the shelf acts as a weak source of CO_2 at 0.32 ± 1.5 mol m^{-2} yr^{-1}. Subregions, however, reveal slightly different trends, where surface waters associated with 40–200-m isobath in the northern and southern WFS are generally weak sinks all year, except for summer when they act as sources of CO_2. Conversely, nearshore waters (<40 m) are a source of CO_2, particularly the southern shallow waters, which are a source all year round. The pCO_2 of seawater has been increasing at a rate of approximately 4.37 μatm/year as compared to atmospheric pCO_2 which has increased at a rate of about 1.7 μatm per year from 1996 to 2016. The annual CO_2 flux has increased from −0.78 to 0.92 mol m^{-2} yr^{-1} on the shelf from 1996–2016. The WFS is emitting 9.23 Tg C/year, with the southern nearshore region emitting the most at 9.01 Tg C/year and the northern region acting as a sink of −1.96 Tg C/year. Aragonite saturation state on the WFS shows seasonal and geographic trends with values ranging from 2 to 5. Lowest values are found in winter associated with subregion <40-m isobath.

Plain Language Summary The West Florida Shelf (WFS) is a source of uncertainty for determining the Gulf of Mexico carbon budget and how surface waters are being affected by increasing atmospheric carbon dioxide (CO_2) levels. Little is known about the WFS trends of the seawater partial pressure of carbon dioxide (pCO_2) over the last decades; much of the uncertainty stems from lack of data. In order to address some of this uncertainty, approximately 135,000 pCO_2 values collected on 97 research cruises between 1996 and 2016 were analyzed and show that the shelf waters have changed from being a weak sink to weak source of CO_2 to the atmosphere. Further, data was divided into four geographical subregions. Offshore surface waters absorb CO_2, whereas nearshore surface waters emit CO_2 to the atmosphere. Importantly, pCO_2 of the nearshore seawater has been increasing at a rate approximately 2.5 times faster than atmospheric pCO_2 over the past 20 years. These data indicate that factors in addition to the atmosphere CO_2 are influencing increases in nearshore seawater. Additionally, WFS aragonite saturation state, often used to monitor ocean acidification conditions, shows seasonal and geographic trends, with year-round supersaturated values ranging from 2 to 5.

1. Introduction

1.1. Background

The Gulf of Mexico (GOM) is a large semienclosed subtropical/tropical sea shared almost equally by the United States and Mexico. The drainage basin of the GOM contains 33 major river systems and extends over approximately 40% of the contiguous U.S. landmass. The GOM was identified as the single largest source of uncertainty in the North American carbon budget by the first State of the Carbon Cycle Report (SOCCR; Chavez et al., 2007). To address this uncertainty, a considerable number of observations have been made in recent years, particularly in the northern and eastern Gulf coastal regions (e.g., Cai, 2003; Chen et al., 2016; Huang et al., 2015; Lohrenz et al., 2018; Robbins et al., 2014; Xue et al., 2016). However, large areas remain under sampled and poorly characterized in terms of air-sea exchange of carbon dioxide (CO_2), associated carbon fluxes and their variability, and controlling mechanisms. The importance of constraining CO_2 fluxes in the GOM is evident in its effect on the modulation and estimation of continental (atmospheric) CO_2 concentrations as the GOM is one entrance route for North America air mass. Large variabilities between

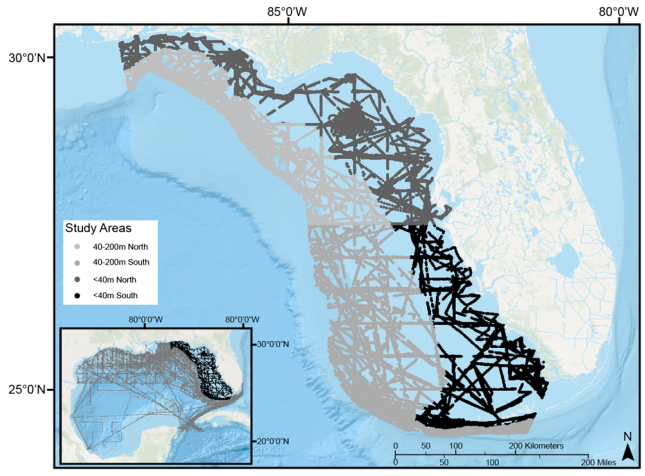

Figure 1. Map of the study area and data points compiled from 97 cruises on the West Florida Shelf. Geographic subregions shaded in different colors. Insert shows cruise track lines from compilation of Gulf of Mexico data from 1996 to 2016.

marine air concentrations in the GOM and continental air masses can introduce significant errors into continental CO_2 fluxes calculated using atmospheric measurements and inversion methods, particularly at regional scales (Peters et al., 2007; Sweeney et al., 2015).

Synthesis efforts suggest that the GOM air-sea CO_2 flux may dominate the net flux of the entire North American margin because of the GOM's large size and strong signals (Chavez et al., 2007). The GOM is one of several large, low-latitude marginal seas in the world's oceans. Water enters the GOM from the Caribbean and exit water becomes part of the larger Gulf Stream system. Northern GOM water is a strong local CO_2 sink due to high primary productivity stimulated by river input of anthropogenically produced nutrients (fertilizers) from the North American continent (Cai, 2003; Chavez et al., 2007; Huang et al., 2015; Lohrenz et al., 2018; Xue et al., 2016). However, while the northern GOM is distinctive in terms of its large river and estuarine-dominated shelf, to the southeast, the West Florida Shelf (WFS) is also distinctive because of the wide, gently sloping rim-to-ramp carbonate platform (<1:2,000 gradient; Hine et al., 2003), substantially less fluvial influence, and significant groundwater input (Smith & Swarzenski, 2012). Previous observational CO_2 flux data suggest an opposite trend on the WFS from the northern GOM: the WFS region acts as a CO_2 source to the atmosphere (Robbins et al., 2014; Xue et al., 2016); however, there is a lack of information about trends in its different subregions. Changes in inorganic carbon in the water concomitantly induce changes in the saturation state (Ω), an indicator of ocean acidification. Wanninkhof et al. (2015) showed general aragonite Ω (Ω_{ar}) trends on the WFS from GOMECC cruises and indicated that additional data were needed to address spatial and temporal variability.

1.2. Geographic Setting

Located on the eastern side of the GOM, the WFS is a low bathymetric gradient calcium carbonate platform approximately 250 km wide, with an area of 170,000 km^2 (Read, 1985; Figure 1). The WFS spans a large latitudinal gradient, from the Florida Panhandle (~30°N) in the north to the Florida Keys (~24°N) in the south. The coastal WFS is characterized by coastal marshes and limestone outcrops in the north, siliciclastic barrier islands in the central region, and mangrove islands and carbonate sediments in the south (Robbins et al., 2009).

The current status of the variability of air-sea CO_2 fluxes on the WFS is not fully known and represents a significant knowledge gap that is critical to our understanding of the carbon cycle and budget in the GOM and over the North America continent, and also how this shelf is responding to climate and anthropogenic changes. In addition, the investigation of the impacts of changing seawater chemistry on habitats in Florida's coastal waters is important to available resources, particularly marine organisms that will be affected by increasing ocean acidification.

In this study, we compiled seawater data from 97 cruises over the last 20 years to determine the spatial and temporal distributions of seawater partial pressure of carbon dioxide (pCO_2) over the WFS and defined subregions. We then quantified the air-sea CO_2 fluxes and identified physical and biogeochemical processes that can control these fluxes. Comparisons of pCO_2 values and fluxes between different subregions and by season were investigated, as well as put in relation with other estimates in the GOM. Finally, WFS Ω_{ar} data were calculated to provide a synoptic evaluation of regional and subregional spatial and seasonal trends. This study provides new information on specifics of pCO_2 distribution and fluxes over the WFS and a conceptual model to illustrate the mechanisms that likely control surface water CO_2 dynamics.

2. Methods

2.1. Database Compilation

The partial pressure of carbon dioxide (pCO_2) data from cruises in the GOM were compiled as part of a large synthesis effort related to the NASA ROSES "Air-Sea CO_2 Flux and Carbon Budget Synthesis and Modeling in

Table 1
Summary of Data Collected on Cruises on the West Florida Shelf

Year	Number of cruises (N = 97)	Data points collected (N = 134,579)	Months											
			January	February	March	April	May	June	July	August	September	October	November	December
1996	2	3,373			•	•								
1997	1	8											•	
2003	4	1,044								•	•			
2006	2	320						•	•					
2007	3	619						•	•	•				
2008	7	20,669				•	•			•	•		•	
2009	10	19,762		•			•	•	•	•	•		•	
2010	8	6,023			•	•	•				•	•		•
2011	9	6,644				•	•	•	•		•	•	•	•
2012	16	18,651		•		•	•	•	•	•	•		•	
2013	5	11,436			•	•	•			•				•
2014	9	8,244				•		•	•		•			•
2015	15	34,489			•	•	•	•	•	•	•	•	•	
2016	6	3,377	•		•	•	•							

the Entire Gulf of Mexico" project. Data were collected from individual cruises and were submitted to publicly available data sets and repositories such as NCEI and SOCAT (Bakker et al., 2017). We analyzed a subset of the data, centered on the WFS, which included 97 WFS research cruises spanning over 20 years (1996, 1997, 2003, 2006–2016) and containing more than 134,000 data points (Table 1). Links to each of the cruise's metadata are found in the supporting information (Table S1). All data had been QA/QC'd prior to being submitted to the repositories and questionable data flagged. Any flagged data and additional records with abnormally high pCO_2 (e.g., >10,000 μatm) or temperature and salinity values out of appropriate ranges, suggesting equipment failure, were not used. These constituted less than 1% of the data.

2.2. Air-Sea Flux Calculations

The air-sea CO_2 flux for the WFS was calculated using a computed second moment of monthly Cross-Calibrated Multiplatform (CCMP) wind speeds (Atlas et al., 2011), thereby taking advantage of the high-resolution winds to appropriately address nonlinearities. The following bulk flux equation (Wanninkhof, 2014) was used to derive air-sea CO_2 fluxes:

$$F = k{\cdot}s{\cdot}\Delta pCO_2$$

where k is the gas transfer velocity, s is the gas solubility (mol L^{-1} atm^{-1}; Weiss, 1974), and ΔpCO_2 is the difference between the air and water pCO_2 values at the respective sites. An $F > 0$ represents emissions of seawater pCO_2 to the air. To determine k at in situ conditions, we used the following:

$$k = k_{660}(Sc_{CO2}/660)^{-0.5}$$

where Sc_{CO2} for CO_2 in seawater is related to temperature by

$$Sc_{CO2} = 2116.8 - 136.25 \times SST + 4.7353 \times SST^2 - 0.092307 \times SST^3 + 0.0007555 \times SST^4$$

and k_{660} is the gas transfer velocity for a gas, parameterized as $k_{660} = 0.251 \times \langle u^2 \rangle$ (Wanninkhof, 2014), where $\langle u^2 \rangle$ is the raw second moment of CCMP wind speeds (Atlas et al., 2011).

Atmospheric pCO_2 was obtained from NOAA Earth System Research Laboratory Globalview-CO_2 (Dlugokencky et al., 2016) for Key Biscayne, FL. The second moment of the winds was obtained from scalar winds from the Cross-Calibrated Multi-Platform (CCMP) wind product at 6-hourly intervals on a 0.5° by 0.5° grid (http://www.remss.com/measurements/ccmp).

2.3. Seasonal pCO_2, CO_2 Fluxes, and Ω_{ar} on the WFS

To evaluate seasonal trends, we grouped data by traditional seasons, whereby winter included cruises during December, January, and February; spring included March, April, and May; summer included June, July, and August; and fall included September, October, and November. Aragonite saturation state (Ω_{ar}) plots were constructed for optimized conditions using the variational method within the Data-Interpolating Variational Analysis (Troupin et al., 2012) as applied in Ocean Data View (Schlitzer, 2017).

2.4. Saturation State Model Using SABGOM

Out of the 97 cruises analyzed, less than 10% measured an additional inorganic carbon parameter besides pCO_2. Therefore, it was challenging to calculate and subsequently evaluate the Ω_{ar} of the WFS without two parameters for calculation. Using data from the few cruises for which alkalinity had been collected, we modeled the total alkalinity (mTA) on the WFS using the SABGOM model, which is a physical-biogeochemical coupled model, covering the South Atlantic Bight and the entire GOM domain. The physical model adopted for SABGOM is the Regional Ocean Modeling System (ROMS). It has a horizontal grid at 5-km resolution and 36 terrain-fellow vertical layers. A biogeochemical model, described in Fennel et al. (2006, 2008), was coupled with the physical (ocean circulation) model. The biogeochemical model consists of a nitrogen cycling model and a carbon cycling model. Both physical and biogeochemical models in SABGOM were well validated by comparing surface elevation, SST, salinity, nitrate, chlorophyll, and pCO_2 with observations (Xue et al., 2013, 2016). With SABGOM, a seven-year (2004–2010) hindcast simulation was applied. The mTA (47,256 data points) was interpolated to nearby stations in this study. mTA and the corresponding measured pCO_2 value at that location were then used to calculate Ω_{ar} using CO2calc v.4.0.9 (Robbins et al., 2010) with the carbonic acid dissociation constants K1 and K2 from Millero (2010), the dissociation constant for HSO_4 from Dickson (1990), and the borate-salinity relationship of Lee et al. (2010).

2.5. Statistical Analysis

The pCO_2 and CO_2 flux data were statistically analyzed to determine trends between geographic subregions and seasons. Given the scarcity of data on certain seasons/years and the uneven geographical distribution of the data points, these trends will need to be confirmed or updated with additional data as it continues to be collected. The large latitudinal and longitudinal temperature and salinity gradients on the WFS indicated that the shelf could be subdivided into at least four general subregions. Temperature and salinity data distribution from the four subregions did not follow normal distributions and the nonnormal distributions were not similar; therefore, the Mood median test was applied across the different subregions to statistically verify their distinction. The 40-m isobath was used to delineate the WFS into northern, offshore 40–200 m (ND); northern, nearshore $<$40 m (NS); southern, offshore 40–200 m (SD); and southern, nearshore $<$40 m (SS) subregions (Figure 1). The northern subregion was demarcated from the southern at 27.5°N latitude. Correlation coefficients were calculated to evaluate possible relationships between pCO_2 and temperature. The significance of a relationship was evaluated at $\alpha = 0.05$. Linear regressions were used to assess temporal trends for pCO_2 and CO_2 flux. Mean, standard deviation, and mean CO_2 flux rates were calculated for the seasonally aggregated data points. A seasonally weighted flux for the WFS was converted into $mol \cdot m^{-2} \cdot yr^{-1}$. All statistical analyses were performed with Minitab (v.17.1; State College, PA).

2.6. Complementary Data: Discrete Sampling of Carbonate Parameters

Carbonate chemical parameters analyzed from discrete water samples collected during a variety of cruises were used for verification of pCO_2 and air-sea CO_2 flux trends, as well as for calculation of aragonite saturation state (Ω_{ar}). Water chemistry data collected during studies of offshore freshwater springs along the WFS were used to investigate pCO_2 and CO_2 flux in this study**.** These springs data were collected at Crystal Beach Spring in Saint Joseph Sound north of Clearwater, FL (28.0843°N, −82.7847°W) at the vent (8.85 m below surface seawater) and surface (0.5 m) on 23 June 2009. Temperature and salinity were recorded using a YSI 3200 conductivity instrument. Wind speed at the time of collection was 1.3 m/s (Clearwater Met station for 23 June 2009). Borosilicate glass bottles (300 ML, Wheaton Industries, Inc., USA) were used to collect seawater to analyze for dissolved inorganic carbon (DIC) and total alkalinity (TA). These were poisoned with $HgCl_2$. The DIC and TA analyses were performed at the USGS Carbon Laboratory, St. Petersburg, FL, using an Ocean Optics USB 2000 spectrophotometer and an UIC Model CM5014 CO_2 coulometer with Model

Table 2
Yearly Mean pCO_2 and CO_2 Flux Rates During West Florida Shelf Cruises

Year	pCO_2 (μatm)	CO_2 flux (mol·m^{-2}·yr^{-1})
1996	315.5 ± 11.7	−0.78 ± 0.20
1997	347.1 ± 0.6	−0.24 ± 0.02
2003	373.4 ± 14.6	0.30 ± 0.30
2006	380.9 ± 53.3	0.48 ± 0.70
2007	429.1 ± 79.3	0.60 ± 0.70
2008	369.0 ± 31.5	−0.26 ± 0.90
2009	384.3 ± 50.7	−0.02 ± 1.20
2010	390.5 ± 23.9	0.41 ± 0.65
2011	406.9 ± 74.4	0.55 ± 1.80
2012	440.6 ± 97.6	1.28 ± 2.50
2013	392.6 ± 20.3	0.19 ± 0.64
2014	397.0 ± 34.8	0.09 ± 0.90
2015	413.2 ± 58.9	0.44 ± 1.25
2016	425.9 ± 45.1	0.92 ± 1.40

CM5130 Acidification Module. Analytical methods were derived from Yao and Byrne (1998), DOE (1994), and Dickson et al. (2007) and used certified reference materials from A. Dickson (Scripps Institution of Oceanography). The precision of DIC and TA was determined to be ±0.1%. pCO_2 was calculated from DIC and TA using CO_2calc v.4.0.9 using previously described constants.

3. Results

Table 1 lists a summary of the number of cruises, data points, months, and years of data. Yearly means for pCO_2 and CO_2 flux ± one standard deviation for years 1996–2016 were calculated for the entire WFS (Table 2). These data demonstrate the level of interannual variability in pCO_2 values and that overall the WFS has been a small net source of CO_2 to the atmosphere since 2010. Mean values for the entire WFS are 399.5 μatm and 0.32 mol·m^{-2}·yr^{-1} for pCO_2 and CO_2 flux, respectively.

3.1. Geographic and Seasonal Distribution of pCO_2 and CO_2 Flux

Mean values of pCO_2 and CO_2 flux for subregions show that northern subregions (ND and NS) have values that are lower than those observed in the south (SD and SS; Table 3). Seasonal pCO_2 (Figure 2) and CO_2 flux (Figure 3) for geographic subregions show general decreasing values from nearshore to offshore and distinct seasonal differences (Table 4).

Winter and spring mean CO_2 flux values in the nearshore shallow northern WFS surface water are negative (−0.66 and −0.65 mol·m^{-2}·yr^{-1}, respectively) and are positive in summer and fall (0.79 and 0.90 mol·m^{-2}·yr^{-1}, respectively). In the offshore deeper (40–200 m) waters in the northern and southern WFS, CO_2 flux values are negative for most of the year, except during summer when, on average, they are positive.

The pCO_2 data are significantly and more strongly correlated with temperature in northern offshore and nearshore surface waters (r = 0.680 (ND), r = 0.671 (NS)) than in southern offshore and nearshore surface waters (r = 0.14 (SS), r = 0.349 (SD)).

3.2. Yearly Trends

Seawater pCO_2 values show a general increase of 4.37 μatm/year (r^2 = 0.65, $p < 0.001$), while the atmospheric pCO_2 is increasing at 1.7 μatm/year (r^2 = 0.90, $p \leq 0.001$; Figure 4a). The linear trend of surface seawater pCO_2 from each geographic subregion is significantly different from the others. Concomitantly, mean CO_2 flux has been increasing about 0.054 mol·m^{-2}·yr^{-1} (r^2 = 0.43, $p < 0.001$) for the entire WFS since 1995 (Figure 5a). Each subregion also shows statistically important yearly increases except for SS (0.028 mol·m^{-2}·yr^{-1}; r^2 = 0.005, p = 0.39). The increases for SD were 0.0262 mol·m^{-2}·yr^{-1} (r^2 = 0.107, $p < 0.001$), NS at 0.047 mol·m^{-2}·yr^{-1} (r^2 = 0.276, $p < 0.001$), and ND at 0.0287 mol·m^{-2}·yr^{-1} (r^2 = 0.163, $p < 0.001$; Figure 5b).

A comparison of yearly pCO_2 data from each subregion for the month of April showed an increase from earlier cruise years to later years (Table 5). April data were chosen because they represented the largest span of

Table 3
Mean Values of pCO_2 and CO_2 Flux for West Florida Shelf Subregions

Subregion	Water depth (m)	Subregion label	Data points collected	pCO_2 mean (μatm)	CO_2 flux mean (mol·m^{-2}·yr^{-1})
North of 27.5°N	<40	NS	21,158	387.3 ± 63.9	0.10 ± 1.3
North of 27.5°N	40–200	ND	31,341	375.0 ± 27.3	−0.20 ± 0.7
South of 27.5°N	<40	SS	31,289	445.7 ± 86.6	1.30 ± 2.1
South of 27.5°N	40–200	SD	50,791	391.1 ± 42.0	0.15 ± 1.1
All subregions			134,579	399.5 ± 62.5	0.32 ± 1.5

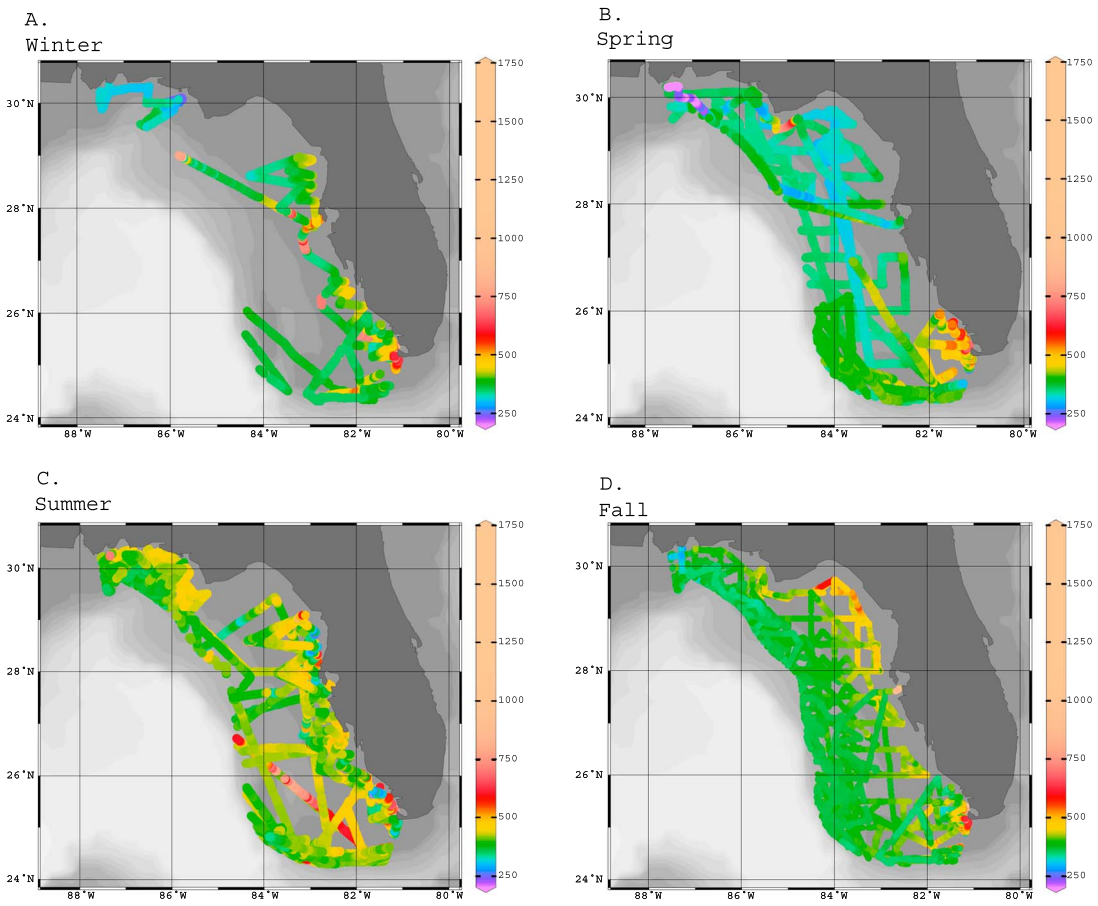

Figure 2. pCO_2 values (μatm) for the West Florida Shelf during the (a) winter, (b) spring, (c) summer, and (d) fall seasons.

early and later years and contained cruises from all the subregions. In 1996, mean pCO_2 of ND surface water was 309.8 μatm, while in 2013, it was 358.0 μatm. CO_2 flux to the atmosphere increased during these years (seawater became less of a sink of CO_2), with seawater pCO_2 increasing at a greater rate than atmospheric pCO_2. These trends generally were observed in all geographic subregions. However, SD had more years of data collected (total of nine) than the rest of the geographic subregions and showed more variability of pCO_2 from year to year.

3.3. Saturation State

Aragonite saturation state on the WFS varies by location and by season. The heterogeneity of coastal waters' saturation state is reflected in values ranging from 2 to 5. Northern WFS Ω_{ar} averages ~3.71 to 3.75, while coastal locations within the 40-m isobath show lower values, with the lowest values associated with the Florida Spring coast and in the Florida Panhandle in January (~2.4). Seasonally, the lowest values are found in coastal waters in winter with higher Ω_{ar} in localized areas. Highest Ω_{ar} values are found in September, generally over 3.5, and with small areas of lower Ω_{ar} (Figures 6a–6d). By November, Ω_{ar} increases from nearshore to offshore (from $<$3.2 nearshore to ~4 in the open GOM).

Subregions ND and SD have mean Ω_{ar} values of 3.71 ± 0.24 and 3.76 ± 0.30, respectively. SS and NS show mean Ω_{ar} values of 3.45 ± 0.45 and 3.41 ± 0.42, respectively. NS has a distinctive bimodal distribution of Ω_{ar} data where the lower mode at ~3 is associated with the Florida Springs coast. A low mean Ω_{ar} value of 3.06 is also seen at the surface of Crystal Beach Spring where surface pCO_2 values are higher than offshore values (Table 6).

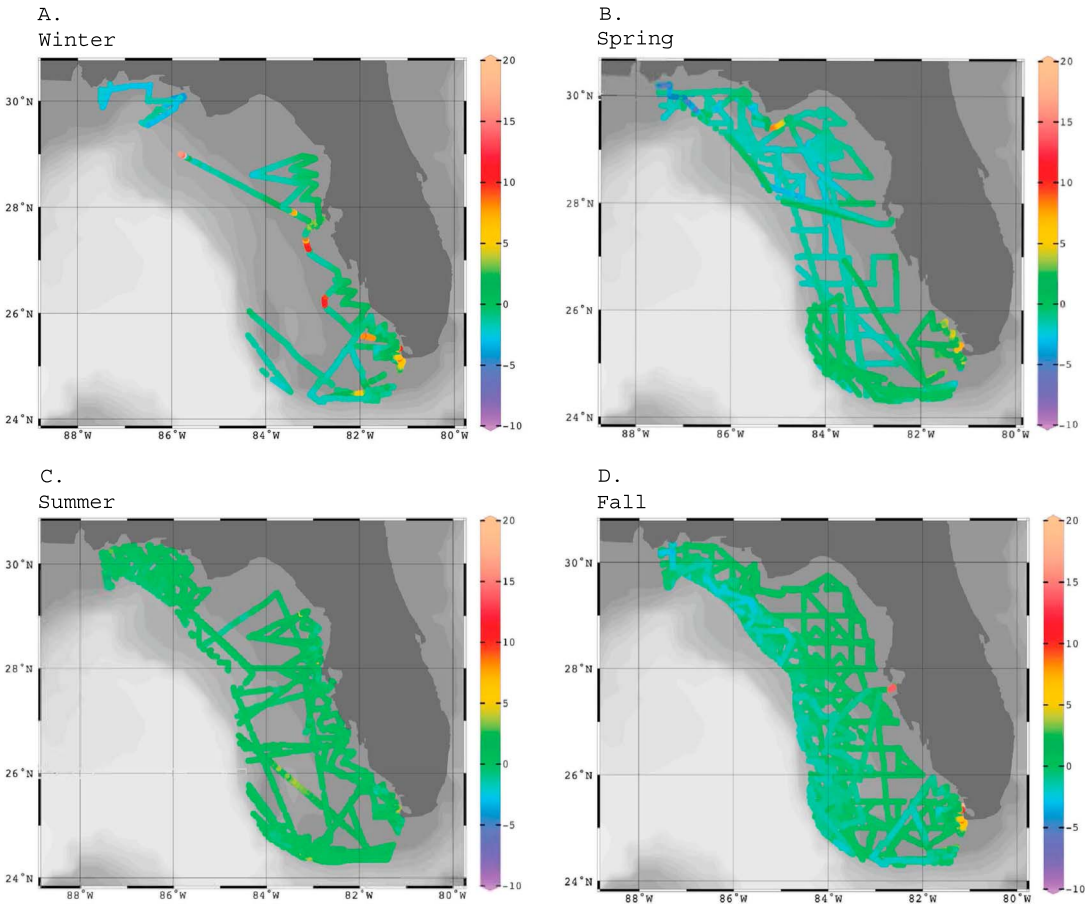

Figure 3. CO_2 flux values (mol m^{-2} yr^{-1}) for the West Florida Shelf during the (a) winter, (b) spring, (c) summer, and (d) fall seasons.

Table 4
Mean Surface pCO_2 and CO_2 Flux Rates Per Season and Subregion for the West Florida Shelf

Season	Subregion	Water depth (m)	Subregion label	Data points collected	pCO_2 (μatm)	CO_2 flux (mol·m^{-2} yr^{-1})
Winter	North of 27.5°N	<40	NS	1,435	365.0 ± 73.0	−0.66 ± 1.9
	North of 27.5°N	40–200	ND	336	364.7 ± 67.7	−0.76 ± 2.5
	South of 27.5°N	<40	SS	5,207	417.6 ± 76.9	0.87 ± 2.1
	South of 27.5°N	40–200	SD	1,132	372.6 ± 26.7	−0.86 ± 0.9
Spring	North of 27.5°N	<40	NS	9,119	344.7 ± 38.1	−0.65 ± 0.6
	North of 27.5°N	40–200	ND	6,889	347.9 ± 21.4	−0.93 ± 0.6
	South of 27.5°N	<40	SS	7,921	431.2 ± 62.7	0.75 ± 1.3
	South of 27.5°N	40–200	SD	14,678	382.1 ± 24.4	−0.17 ± 0.6
Summer	North of 27.5°N	<40	NS	4,982	427.0 ± 59.3	0.79 ± 1.0
	North of 27.5°N	40–200	ND	8,101	400.9 ± 22.6	0.33 ± 0.4
	South of 27.5°N	<40	SS	9,365	468.1 ± 102.5	1.71 ± 2.5
	South of 27.5°N	40–200	SD	16,484	413.3 ± 61.1	0.68 ± 1.5
Fall	North of 27.5°N	<40	NS	5,622	426.9 ± 50.1	0.90 ± 1.1
	North of 27.5°N	40–200	ND	16,015	373.8 ± 15.7	−0.15 ± 0.6
	South of 27.5°N	<40	SS	8,796	451.5 ± 85.1	1.48 ± 2.2
	South of 27.5°N	40–200	SD	18,497	379.6 ± 18.1	−0.02 ± 0.5

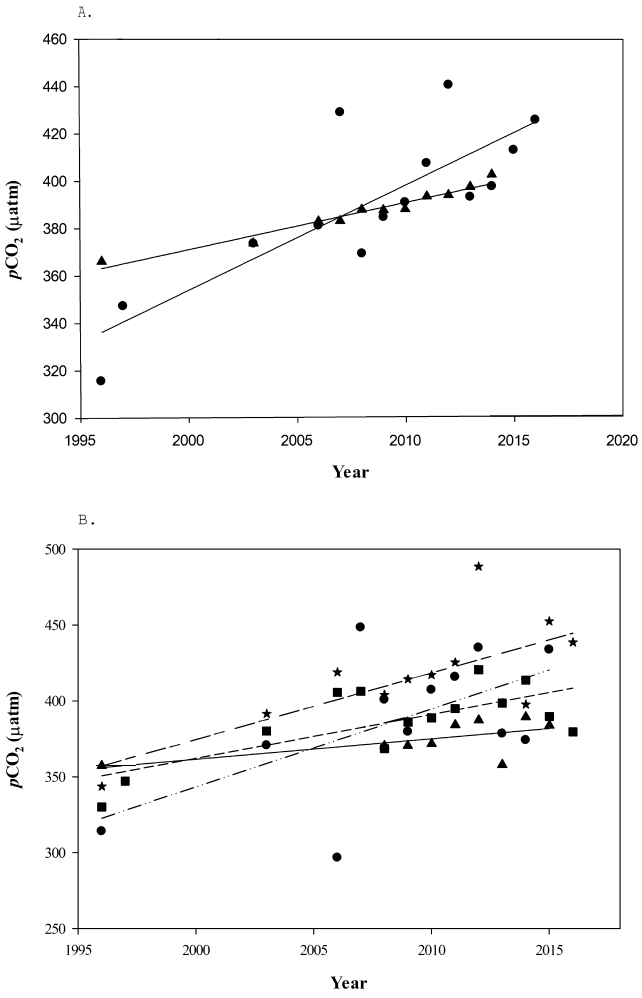

Figure 4. Yearly mean pCO_2 values and linear regression models for (a) CO_{2air} (black triangle) and CO_{2sw} (black circle) and (b) from locations and depths of north of 27.5°N and 40–200 m (black triangle, solid line) north of 27.5°N and <40 m (black circle, dashed and dotted line) south of 27.5°N and 40–200 m (black square, short-dashed line) and south of 27.5°N and <40 m (black star, long- and short-dashed line) on the West Florida Shelf.

4. Discussion

4.1. Controlling Factors of pCO_2 and Carbon Flux Distributions

The compilation of more than two decades of pCO_2 data collected from waters over the WFS provides a basis to observe general trends, evaluate processes that control carbon fluxes, and further investigation into potential ocean acidification impacts on this wide continental shelf and coastal area. The temperature gradients from north to south, coastal to offshore, and seasonally are broad-scale drivers in the variability of pCO_2 and carbon emissions over the year. The stronger correlations of pCO_2 to temperature in the northern subregions versus the southern subregions are likely consequences of more dramatic seasonal temperature swings in the north compared to the south. However, in the offshore southern subregions, pCO_2 is more strongly controlled by temperature than in nearshore waters, where increased photosynthesis followed by respiration, as a result of terrestrial inputs of nutrients, is well documented (Bergamaschi et al., 2012; Bianchi et al., 2010; Turner et al., 2006). Additionally, processes such as Gulf Stream loop current (Wanninkhof et al., 2015), river input, localized plankton blooms, enhanced primary productivity, and nearshore submarine groundwater discharge (Smith & Robbins, 2012) and river runoff (Ho et al., 2017) can play a significantly larger role in influencing pCO_2 values.

Our findings confirm earlier studies that indicate that the WFS has small CO_2 fluxes on the shelf, with the surface water overall acting as either a weak source or sink of carbon for most of the year (Robbins et al., 2014; Xue et al., 2016). In contrast to the northern deeper water subregion which generally acts as a weak sink of CO_2, similar to its northern neighbor the north Gulf of Mexico (Huang et al., 2015), the other subregions act as weak sources, depending on season. Surface pCO_2 on the WFS is variable both spatially and seasonally but overall, the shelf is nearly in equilibrium with the atmosphere for most of the year. Areas of relatively larger positive and negative fluxes are found in specific areas that coincide with nearshore freshwater springs, upwelling localities, mouths of estuaries, and Everglades riverine runoff (Ho et al., 2017). Ephemeral plankton blooms and other physio-biological processes, such as photosynthesis, respiration, and remineralization, also cause enhanced fluxes (Cai, 2011). While north to south and west to east increasing CO_2 flux trends on the shelf partially reflect increasing temperatures, this influence breaks down in SS, the shallowest and most southern subregion, where the correlation between temperature and flux, although significant, is not strong.

Clearly, more data are needed to fully understand what controls the trends in each of the subregions. For example, terrestrial and atmospheric anthropogenic processes (e.g., increased nutrient loadings, proximity to urbanization, CO_2 release from vehicles, and power plant emissions) and the consequences of these are influencing much of the coastal and estuarine ecosystems. Adding to the complexity of the general coastal influences is the outflow of major and minor estuaries along the WFS. Not surprisingly, Tampa Bay shows significantly different pCO_2 and CO_2 flux signals compared to adjacent shelf areas, particularly in the fall (Figures 2d and 3d). Importantly, estuaries along the west coast of Florida, including Tampa Bay, and other smaller estuaries along the coast, such as St. Josephs, Citrus County, Cedar Key, and Ten Thousand Islands, all demonstrated significant pH and oxygen decreases over the last 30 years, which affect the nearshore chemistry (Robbins & Lisle, 2017). In addition to submarine groundwater discharge and nearshore and freshwater seeps, plankton blooms and benthic vegetation, storms and upwelling events, and $CaCO_3$ precipitation in the nearshore also are driving processes that can modulate the CO_2 flux values.

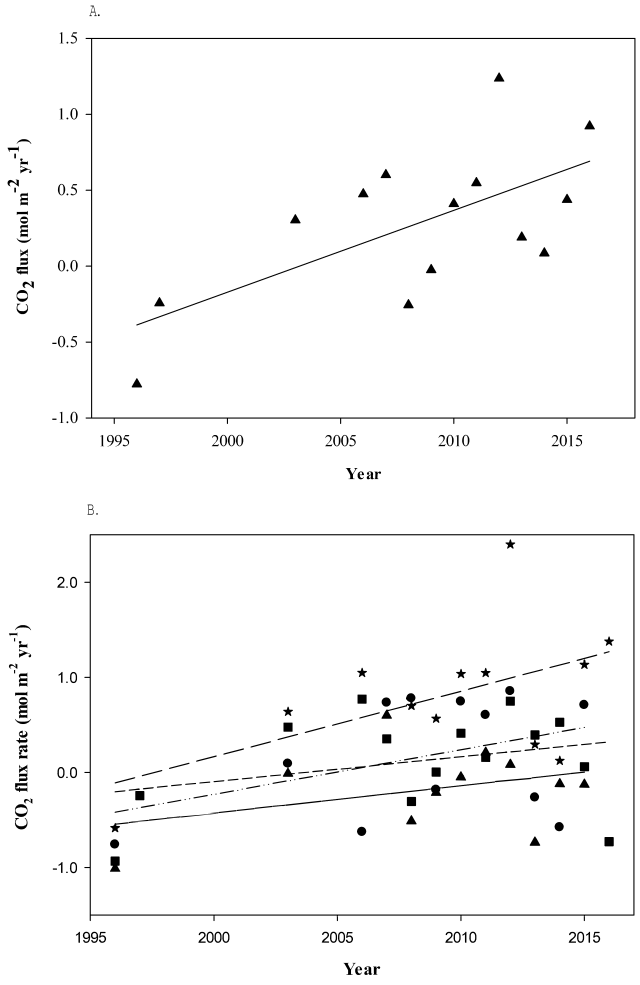

Figure 5. Yearly mean CO_2 flux values and linear regression models for (a) the entire West Florida Shelf and (b) from locations and depths of north at 40–200 m (black triangle, solid line), north <40 m (black circle, dashed and dotted line), south of 27.5°N and 40–200 m (black square, short-dashed line) and south of 27.5°N and <40 m (black star, long- and short-dashed line) on the West Florida Shelf.

Terrestrial inputs of carbon onto the WFS include discharges from local rivers and submarine springs. Eight rivers and associated estuaries, as well as coastal and offshore groundwater seeps (Barrera & Robbins, 2017; Santos et al., 2008; Smith & Robbins, 2012), influence the WFS carbon budget. However, the influence of nearshore waters mixing with river discharge on carbon is relatively minimal compared to that in the Mississippi River region; instead, the carbon budget is driven by microbial processes (Wang et al., 2013). In addition to the Mississippi River, the two major rivers affecting the northern WFS are the Suwannee and Apalachicola Rivers. On the southern part of the WFS, only small rivers drain low-relief basins (Boning, 2007) including the Everglades National Park which has several smaller outflows discharging significant amounts of inorganic carbon onto the shelf (Bergamaschi et al., 2014, Ho et al., 2017).

Submarine groundwater discharges (SGD) associated with nearshore and offshore sink holes and nonpoint source discharges locally influence pCO_2, CO_2 flux, and saturation state. Visually, the influence of the springs on the coast during the summer and winter is apparent in remotely sensed temperature images, where relatively warmer fresh spring waters can be observed in the winter surrounded by cooler marine waters (Raabe et al., 2011). Geochemically, the discharges of nearshore springs impact local geochemistry of the seawater as seen at two coastal sites associated with Homosassa springs in 2008, which showed CO_2 fluxes of over 819 kg C/year (68250 mol/year) and pCO_2 values of up to 1,814 μatm (Barrera & Robbins, 2017). Cruises during August 2008 and February 2009 in this area recorded values of relatively increased pCO_2 and lower salinities compared to surrounding waters. Another example of a nearshore coastal spring that is influencing nearshore geochemistry is Crystal Beach Spring, which is one of the largest springs on the WFS that discharge significant volumes of relatively fresh groundwater (Table 6). Smith and Swarzenski (2012) calculated SGD rates conservatively to be between 0.7 and 3.5 cm/day. In areas associated with spring and submarine groundwater, these discharges are associated with higher pCO_2 and lower Ω_{ar}. For example, in NS, the lowest Ω_{ar} values are located near the Florida Springs Coast, and higher Ω_{ar} values are located near the Florida Panhandle and other northern areas.

In the SS subregion (southern WFS < 40 m), pCO_2 values are generally the highest compared to the other subregions. While temperature is one of the controlling factors, it only accounts for 14% of the association. Other factors such as nearshore springs mixing with shallow waters, water outflow from Everglades National Park (Ho et al., 2017) onto the WFS, and general calcification of organisms and sediments on the WFS, likely influence pCO_2 values. Geothermal springs are also present in the southern nearshore WFS, in contrast to the north where more surface expression of the Floridan aquifer system-fed springs are observed. Nearshore geothermal springs discharge in the SS subregion were reported to have pH values lower than the surrounding gulf waters (~7.36 versus 8.25 at 25 °C; Fanning et al., 1981). Acidification of this spring water has been attributed to oxidation of organic matter and precipitation of minerals (Fanning et al., 1981; Schijf & Byrne, 2007). Particulate inorganic carbon in the form of calcium carbonate is more prevalent in the southern GOM, where generally clear, oligotrophic, warm water promotes the development of chlorozoan (calcareous green algae, corals, and mollusks) formed sediments (Hallock et al., 2010; Wilson, 1975). The larger pCO_2 values in SS versus the NS may in part reflect the increases in the biomass of calcium carbonate organisms, diagenetic sediment processes, and other carbonate precipitation processes. For example, a general trend of very high pCO_2 values was observed between 25.272°N and 25.939°N which is also an area recognized by localized calcium carbonate precipitation events associated with diatom blooms (Long et al., 2017). Remote sensing showed enhanced reflectance and backscattering in these features (Long et al., 2014,

Table 5
Mean Surface pCO_2 and CO_2 Flux Rates Per Subregion for April During West Florida Shelf Cruises

Subregion	Water depth (m)	Subregion	Year	Data points collected	pCO_2 (μatm)	CO_2 flux (mol m^{-2} yr^{-1})
North of 27.5°N	<40	NS	1996	3023	314.1 ± 10.7	−0.76 ± 0.20
		NS	2008	625	344.0 ± 5.6	−0.73 ± 0.20
		NS	2013	3185	378.0 ± 10.5	−0.26 ± 0.20
North of 27.5°N	40–200	ND	1996	48	309.8 ± 6.4	−1.01 ± 0.10
		ND	2008	3372	344.7 ± 4.5	−0.90 ± 0.10
		ND	2013	94	358.0 ± 4.5	−0.7 ± 0.10
South of 27.5°N	<40	SS	2014	281	398.9 ± 32.9	0.25 ± 0.90
		SS	2015	3544	443.5 ± 55.7	0.85 ± 0.70
South of 27.5°N	40–200	SD	1996	161	328.6 ± 11.8	−0.74 ± 0.30
		SD	2008	3119	368.4 ± 5.2	−0.31 ± 0.20
		SD	2010	48	380.1 ± 1.2	−0.05 ± 0.03
		SD	2011	67	388.7 ± 1.1	0.14 ± 0.02
		SD	2012	63	376.0 ± 4.8	−0.27 ± 0.20
		SD	2013	133	351.8 ± 4.2	−1.21 ± 0.20
		SD	2014	621	417.9 ± 8.5	0.80 ± 0.25
		SD	2015	320	397.6 ± 6.4	0.14 ± 0.10
		SD	2016	113	380.7 ± 4.9	−0.43 ± 0.20

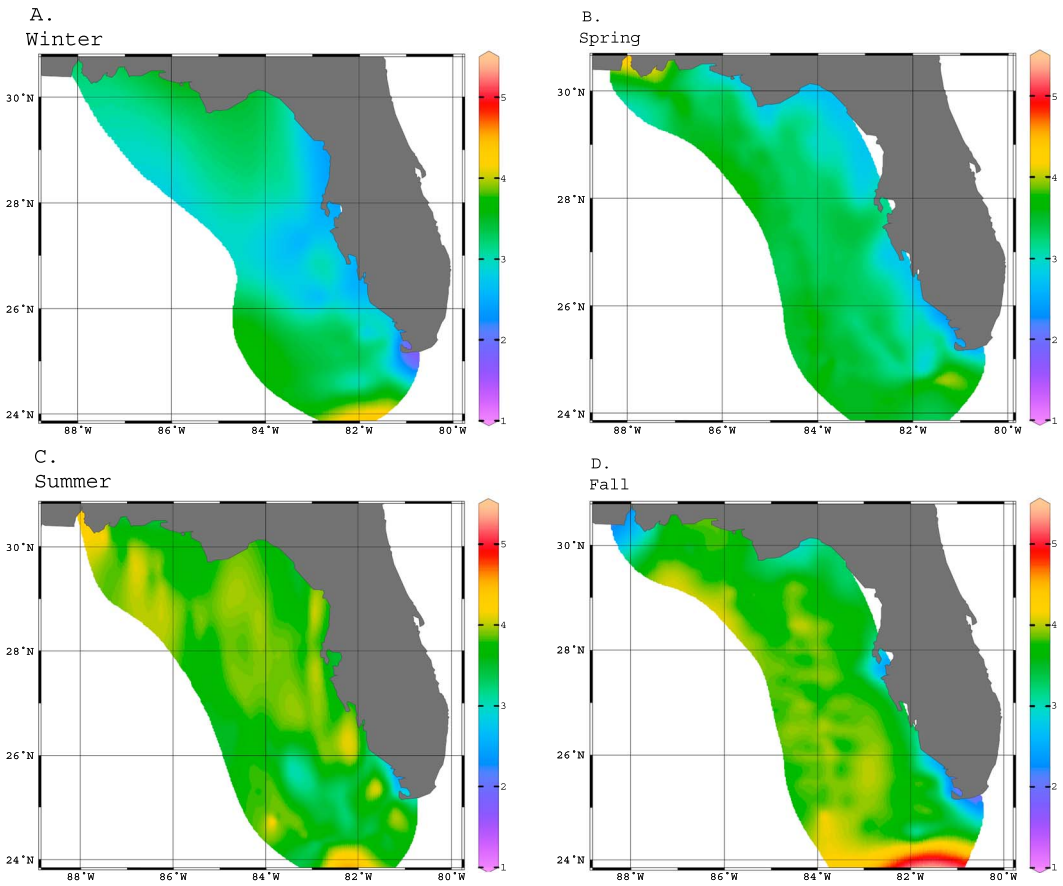

Figure 6. Aragonite saturation states (Ω_{ar}) values for the West Florida Shelf during the (a) winter, (b) spring, (c) summer, and (d) fall seasons.

Table 6
Water Chemistry for Crystal Beach Spring

Sample type	Data points collected	Collection depth (m)	Temperature (°C)	Salinity (PSU)	pH (total scale)	pCO_2 (μatm)	Ω aragonite (unitless)	CO_2 flux (mol m^{-2} yr^{-1})
Discharge vent	5	8.85	19.7 ± 1.2	3.6 ± 0.1	7.15 ± 0.08	8008 ± 1331	0.26 ± 0.07	10.9 ± 1.90
Surface water	3	0.50	15.6 ± 1.4	28.7 ± 4.5	8.0 ± 0.11	588 ± 239	2.92 ± 0.68	0.27 ± 0.31

2017), and the bloom cell concentrations were nearly 5 times higher inside than outside the waters that have high levels of suspended, fine-grained calcium carbonate. MODIS data over a nearshore SS location during a ten-year time span showed a seasonal signal for these events (Long et al., 2017).

4.2. Seasonal and Geographic Trends

These data demonstrate significant spatial and seasonal variations in surface water pCO_2, carbon flux, and Ω_{ar} distributions in waters of the WFS. An increasing latitudinal gradient of pCO_2 from north to south demonstrates that northern sites have lower pCO_2 and lower CO_2 efflux than the more southern sites. Further, pCO_2 and CO_2 flux values show a decreasing coastal to offshore gradient. Seasonality of pCO_2 is observed in mean values, which are comparable to those modeled by others (Chen et al., 2016; Xue et al., 2016). As expected, aragonite saturation state on WFS increases from winter to summer months. Fall data show clear associations between relatively lower Ω_{ar} values in estuaries and coastal zones with offshore waters, suggesting seasonal runoff. The Florida loop current also likely influences the WFS saturation state; however, this cannot be confirmed with the current data set. Saturation state trends demonstrate similar spatial variability and gradients observed in the pCO_2 and carbon flux data, with nearshore having lower saturation state values than offshore sites. Locations with higher temperatures and salinities, such as in the SS, show higher Ω_{ar} values than northern sites. Summertime values are typically higher than in other seasons. Future cruises that fill spatial and seasonal data gaps will improve the saturation state model.

The overall mean trend indicates that the WFS currently fluctuates between being a weak sink and weak source of carbon during the year in ND, NS, and SD. Generally, the WFS is a weak source of CO_2, although it becomes a sink in the spring and winter. The exception to this is the SS, which remains a source of CO_2 all year round and is approximately an order of magnitude higher than in subregions ND, NS, and SD. Calculated CO_2 fluxes corrected for the area for each of the subregions (Table 7) show that overall, the combined flux over the WFS is 9.23 Tg/year and subregion values increase from north to south. Geographically, the ND is a sink of carbon at −1.9 Tg/year in comparison to the other subregions, such as NS, which is a source of carbon at 8.7 Tg/year.

4.3. Long-Term Trends

Seawater pCO_2 values have been steadily increasing from 1996 to 2016, a trend particularly noticeable in the nearshore zone despite temporal and geographical gaps. As a result, the WFS has been a weak source of carbon to the atmosphere (except for the northern 40–200-m subregion), becoming larger over time. These increases not only reflect increasing atmospheric pCO_2 but also reflect additional nearshore processes that are concomitantly occurring faster than global CO_2 increases. The largest change in flux is occurring in the

Table 7
Annual Total Carbon Flux Rates Per Subregion of the West Florida Shelf

Subregion	Water depth (m)	Subregion label	Subregion area (km^2)	Proportion of West Florida Shelf (%)	Annual carbon flux rates (Tg C/year)	Annual carbon flux rates (Tg C yr^{-1} km^{-2})
North of 27.5°N	<40	NS	52,338	30.1	0.87	1.66×10^{-5}
North of 27.5°N	40–200	ND	29,327	16.9	−1.96	-6.68×10^{-5}
South of 27.5°N	<40	SS	42,555	24.5	9.00	2.11×10^{-4}
South of 27.5°N	40–200	SD	49,402	28.5	1.31	2.65×10^{-5}
West Florida Shelf			173,622	100.0	9.22	5.31×10^{-5}

Table 8
North American Regional Studies With Calculations of pCO_2 and/or CO_2 Flux

Region	pCO_2 trend (μatm/year)	Mean CO_2 flux ($mol \cdot m^{-2} yr^{-1}$)	Time period	Data source	Author
SAB[a]	3.0–4.5	ND	1991–2016	In situ pCO_2 (cruises/moorings)	Reimer et al. (2017)
SAB[a]	ND	−0.48 ± 0.21	2005–2006	In situ pCO_2 (cruises)	Jiang et al. (2008)
SAB[a] Inner shelf	ND	1.2 ± 0.24	2005–2006	In situ pCO_2 (cruises)	Jiang et al. (2008)
SAB[a] Outer shelf	ND	−1.34 ± 0.21	2005–2006	In situ pCO_2 (cruises)	Jiang et al. (2008)
Northern GOM[b]	ND	−0.96 ± 3.7	2004–2010	In situ pCO_2 (cruises)	Huang et al. (2015)
Northern GOM[b]	ND	−1.1 ± 0.3	2006–2010	Satellite estimates	Lohrenz et al. (2018)
FGNMS[c]	ND	−0.00014 ± 0.00196	2013–2016	In situ pCO_2 (cruises)	Hu et al. (2018)
Western tropical North Atlantic	1.11 ± 0.35	−0.06 ± 0.18	2002–2009	In situ pCO_2 (cruises)	Park and Wanninkhof (2012)
Northern Hemisphere ocean margins	1.93 ± 1.59	ND	35 years	SOCAT v3	Wang et al. (2017)
MAB[d]	1.93 ± 3.11	ND	35 years	SOCAT v3	Laruelle et al. (2018)
WFS[e] (entire), 0–200 m	4.43	0.32 ± 1.5	1996–2016	In situ pCO_2 (cruises)	This study
WFS subregion[f], north <40 m	5.14	0.10 ± 1.3	1996–2015	In situ pCO_2 (cruises)	This study
WFS subregion, north 40–200 m	1.35	−0.2 ± 0.7	1996–2015	In situ pCO_2 (cruises)	This study
WFS subregion, south <40 m	4.37	1.3 ± 2.1	1996–2016	In situ pCO_2 (cruises)	This study
WFS subregion, south 40–200 m	2.89	0.15 ± 1.1	1996–2016	In situ pCO_2 (cruises)	This study

Note. ND = not determined.
[a]SAB = South Atlantic Bight. [b]GOM = Gulf of Mexico. [c]GNMS = Flower Gardens National Marine Sanctuary. [d]MAB = Mid-Atlantic Bight. [e]WFS = West Florida Shelf. [f]Subregion delineated at 27.5°N as described in section 2.

northern and southern <40-m WFS, where nearshore flux rates to the atmosphere are significantly higher than the offshore rates (Figures 5a and 5b). Mean values between the 1990s and early 2000s are negative, but from 2006 to 2016 are generally positive, with the largest mean flux value being observed in 2012 (Table 2). Given the small subset of data prior to 2006 (4,425 data points in total, or 3.3% of the complete data set), the initial negative mean values may or may not have been representative of the full decade. However, for the fluxes calculated from 2006 onward, while the fluxes are small, the positive trend is statistically significant. Whereas at present we do not have a full explanation why pCO_2 on the WFS, and particularly in nearshore waters, is increasing faster than the atmospheric CO_2 rate of increase, this trend is similar to the trend recently estimated for the South Atlantic Bight (Reimer et al., 2017; Table 8). Such trends may reflect an increase in eutrophication and the terrestrial export of CO_2 and dissolved organic carbon (DOC) into the nearshore (Borges & Gypens, 2010; Jiang et al., 2008). Possible reasons for this export on the WFS may be due to increased land use and land cover changes in the drainage basins and sea level rise mobilizing CO_2 and DOC out of the extensive coastal wetland areas, such as the Florida Everglades. Elsewhere on a global scale, sea surface pCO_2 increase rates in many coastal margins are slower than atmosphere increases (see Laruelle et al., 2018).

In the northern hemisphere, and in coastal areas close to the WFS, sea surface pCO_2 increase rates show a wide range of values (Table 8), as would be expected from the wide variety of physical and chemical settings that investigators have studied, including geographic settings, water masses, chemistry, and temperatures. Furthermore, these studies utilized different time frames in their calculations, from 2 years (Jiang et al., 2008) to 35 years (Laruelle et al., 2018; Wang et al., 2017). And, such as in the research we present, while data may span several decades, there are significant gaps in years when no data were collected. Despite the range of values, similar patterns are observed in the inner and outer shelf of the South Atlantic Bight (Jiang et al., 2008; Table 8) and the nearshore and offshore WFS; both show negative and positive fluxes for these subregional areas, respectively. In the northern Gulf of Mexico, CO_2 flux is small but negative, similar to the northern WFS (Huang et al., 2015; Table 8). CO_2 flux rates for eastern and southern regions of the Gulf of Mexico are the subject of ongoing investigations.

Finally, in spite of the seemingly large data set, there remains a paucity of data within most subregions spatially and seasonally. For example, there are only 336 points representing the outer northern shelf for winter over the 20-year time span. Therefore, along with the natural variability that one would expect to see, the wide variations of values in pCO_2 are reflected in high standard deviations.

5. Summary

Regional monitoring and collecting of carbonate parameters are needed to improve our understanding of ocean processes that impact pCO_2 distributions and fluxes and to promote the development of predictive models of ocean acidification in coastal ecosystems. Here we provide a data synthesis for the WFS that shows significant differences in surface patterns of pCO_2, CO_2 flux, and carbonate saturation state in the context of geographic, seasonal, and interannual variabilities. These data demonstrate that anthropogenic processes are superimposed on natural cycles of CO_2, which have been shifting the ocean chemistry over time. Lack of consistently collected data made interpolations of the data and prediction of future saturation state challenging. Nevertheless, clear incremental increases in atmospheric CO_2 are linked to concomitant increases in pCO_2. The rate of increase, however, is greater than atmospheric increases leading to an increase in CO_2 efflux in the GOM. There are significant subregional and seasonal variations in surface water pCO_2, CO_2 flux, and carbonate saturation state distributions on the WFS. The patterns have provided the basis to identify processes linked to measurable latitudinal, inner to outer shelf, and seasonal changes in coastal and ocean carbon chemistry (pCO_2, CO_2 sea-air flux) and to derive carbonate saturation state maps of Florida shelf waters. Future cruises that target data gaps and uncertainties for pCO_2 and carbonate saturation state are needed for the WFS, where significant declines in carbonate-dominated ecosystems, fishery habitats, and calcifying organisms are predicted for this century. Data are needed to provide fundamental understanding of the coastal carbon cycle and to reveal the processes behind the observations that show that shelf water pCO_2 has increased at a rate faster than the atmospheric rate in the past 20 years.

Acknowledgments

USGS funding for LLR was from the Coastal and Marine Geology Program. Funding for the project was provided by NASA ROSES "Air-Sea CO_2 Flux and Carbon Budget Synthesis and Modeling in the Entire Gulf of Mexico" NNH13ZDA001N for PIs L.L.R., R.H., W.J. C., and L.B. Funding and support from NOAA's Ocean Acidification Program and NOAA's Climate Program Office for data collection on the ships Gordon Gunter, Ronald H. Brown, Walton Smith, Allure of the Seas, and Barcelona Express are also acknowledged. This research was carried out in part under the auspices of the Cooperative Institute for Marine and Atmospheric Studies (CIMAS), a cooperative institute of the University of Miami, and the National Oceanic and Atmospheric Administration, cooperative agreement NA10OAR4320143. Research support was provided by the Florida Institute of Oceanography (FIO)/BP and by the Gulf of Mexico Research Initiative (GOMRI) through C-IMAGE to K.L.D. Data are publicly available (see Table S1 in the supporting information); CTD data are available through the Gulf of Mexico Research Initiative Information and Data Cooperative (GRIIDC) at https://data.gulfresearchinitiative.org (doi:10.7266/N7CC0XN9; 10.7266/N7QR4V28). R.H. and H.Z. also acknowledge funding support from GOMRI, grant 2015-V-487. We thank Joseph Terrano, Ginger Range, and Stephen Douglas for the GIS and ODV assistance. Any use of trade, firm, or product names is for descriptive purposes only and does not imply endorsement by the U.S. Government.

References

Atlas, R., Hoffman, R. N., Ardizzone, J., Leidner, S. M., Jusem, J. C., Smith, D. K., & Gombos, D. (2011). A cross-calibrated, multiplatform ocean surface wind velocity product for meteorological and oceanographic applications. *Bulletin of the American Meteorological Society*, *92*(2), 157–174. https://doi.org/10.1175/2010BAMS2946.1

Bakker, D. C. E., O'Brien, K. M., Pfeil, B., Currie, K. I., Kozyr, A., Landa, C. S., et al. (2017). Surface Ocean CO_2 atlas (SOCAT) v5. *Pangaea*. https://doi.org/10.1594/PANGAEA.877863

Barrera, K. E., & Robbins, L. L. (2017). Historical patterns of acidification and increasing CO_2 flux associated with Florida springs. *Limnology and Oceanography*, *62*(6), 2404–2417. https://doi.org/10.1002/lno.10573

Bergamaschi, B. A., Krabbenhoft, D. P., Aiken, G. R., Patino, E., Rumbold, D. G., & Orem, W. H. (2012). Tidally driven export of dissolved organic carbon, total mercury, and methylmercury from a mangrove-dominated estuary. *Environmental Science & Technology*, *46*(3), 1371–1378. https://doi.org/10.1021/es2029137

Bergamaschi, B. A., Smith, R. A., Sauer, M. J., Shih, J.-S., & Ji, L. (2014). Terrestrial fluxes of nutrients and sediment to coastal waters and their effects on coastal carbon storage in the eastern United States. In Z. Zhiliang & B. C. Reed (Eds.), *Baseline and projected future carbon storage and greenhouse gas fluxes in ecosystems of the eastern United States: U.S. Geological Survey Professional Paper 1804* (Chap. 6, pp. 85–114). https://doi.org/10.3133/pp1804

Bianchi, T. S., DiMarco, S. F., Cowan, J. H. Jr., Hetland, R. D., Chapman, P., Day, J. W., & Allison, M. A. (2010). The science of hypoxia in the northern Gulf of Mexico: A review. *Science of the Total Environment*, *408*(7), 1471–1484. https://doi.org/10.1016/j.scitotenv.2009.11.047

Boning, C. R. (2007). *Florida's Rivers* (p. 256). Sarasota, FL: Pineapple Press.

Borges, A. V., & Gypens, N. (2010). Carbonate chemistry in the coastal zone responds more strongly to eutrophication than ocean acidification. *Limnology and Oceanography*, *55*(1), 346–353. https://doi.org/10.4319/lo.2010.55.1.0346

Cai, W. -J. (2003). Riverine inorganic carbon flux and rate of biological uptake in the Mississippi River plume. *Geophysical Research Letters*, *30*(2), 1032. https://doi.org/10.1029/2002GL016312

Cai, W. -J. (2011). Estuarine and coastal ocean carbon paradox: CO_2 sinks or sites of terrestrial carbon incineration? *Annual Review of Marine Science*, *3*(1), 123–145. https://doi.org/10.1146/annurev-marine-120709-142723

Chavez, F., Takahashi, T., Cai, W.-J., Friederich, G., Hales, B., Wanninkhof, R., & Feely, R. A. (2007). Coastal oceans. In A. W. King, L. Dilling, G. P. Zimmerman, D. M. Fairman, R. A. Houghton, G. Marland, et al. (Eds.), *The First State of the Carbon Cycle Report (SOCCR): The North American Carbon Budget and Implications for the Global Carbon Cycle. A Report by the US Climate Change Science Program and the Subcommittee on Global Change Research* (pp. 149–156), Asheville, NC: National Oceanic and Atmospheric Administration, National Climatic Data Center.

Chen, S., Hu, C., Byrne, R. H., Robbins, L. L., & Yang, B. (2016). Remote estimation of surface pCO_2 on the West Florida Shelf. *Continental Shelf Research*, *128*, 10–25. https://doi.org/10.1016/j.csr.2016.09.004

Dickson, A. G. (1990). Thermodynamics of the dissociation of boric acid in synthetic seawater from 273.15 to 318.15°K. *Deep Sea Research Part A Oceanographic Research Papers*, *37*(5), 755–766. https://doi.org/10.1016/0198-0149(90)90004-F

Dickson, A. G., Sabine, C. L., & Christian, J. R. (2007). Guide to best practices for ocean CO_2 measurements. *PICES Special Publication*, *3*, 191.

Dlugokencky, E. J., Lang, P. M., Mund, J.W., Crotwell, A. M., Crotwell, M. J., & Thoning, K. W. (2016). Atmospheric carbon dioxide dry air mole fractions from the NOAA ESRL carbon cycle cooperative global air sampling network, 1968–2015. Version: 2016-08-30.

DOE (1994). Handbook of methods for the analysis of the various parameters of the carbon dioxide system in sea water, version 2, A. G. Dickson and C. Goyet, eds. Oak Ridge, Tennessee, ORNL/CDIAC-74.

Fanning, K. A., Byrne, R. H., Breland, J. A., Betzer, P. R., Moore, W. S., Elsinger, R. J., & Pyle, T. E. (1981). Geothermal springs of the West Florida continental shelf: Evidence for dolomitization and radionuclide enrichment. *Earth and Planetary Science Letters*, *52*(2), 345–354. https://doi.org/10.1016/0012-821X(81)90188-6

Fennel, K., Wilkin, J., Levin, J., Moisan, J., O'Reilly, J., & Haidvogel, D. (2006). Nitrogen cycling in the middle Atlantic bight: Results from a three-dimensional model and implications for the North Atlantic nitrogen budget. *Global Biogeochemical Cycles*, *20*, GB3007. https://doi.org/10.1029/2005GB002456

Fennel, K., Wilkin, J., Previdi, M., & Najjar, R. (2008). Denitrification effects on air-sea CO_2 flux in the coastal ocean: Simulations for the Northwest North Atlantic. *Geophysical Research Letters*, *35*, L24608. https://doi.org/10.1029/2008GL036147

Hallock, P., Robbins, L., Larson, R., Beck, T., Schwing, P., Martinez-Colon, M., & Gooch, B. (2010). West Florida Shelf: A natural laboratory for the study of ocean acidification. U.S. Geological Survey Open-File Report 2010–1134. Reston, VA: U.S. Geological Survey.

Hine, A. C., Brooks, G. R., Davis, R. A. Jr., Duncan, D. S., Locker, S. D., Twichell, D. C., & Gelfenbaum, G. (2003). The west-Central Florida inner shelf and coastal system: A geologic conceptual overview and introduction to the special issue. *Marine Geology*, *200*(1–4), 1–17. https://doi.org/10.1016/S0025-3227(03)00161-0

Ho, D. T., Ferron, S., Engel, V. C., Anderson, W. T., Swart, P. K., Price, R. M., & Barbero, L. (2017). Dissolved carbon biogeochemistry and export in mangrove-dominated rivers of the Florida Everglades. *Biogeosciences*, *14*(9), 2543–2559. https://doi.org/10.5194/bg-14-2543-2017

Hu, X., Nuttall, M. F., Wang, H., Yao, H., Staryk, C. J., McCutcheon, M. R., et al. (2018). Seasonal variability of carbonate chemistry and decadal changes in waters of a marine sanctuary in the northwestern Gulf of Mexico. *Marine Chemistry*. https://doi.org/10.1016/j.marchem.2018.07.006

Huang, W. J., Cai, W. -J., Wang, Y., Lohrenz, S. E., & Murrell, M. C. (2015). The carbon dioxide system on the Mississippi River-dominated continental shelf in the northern Gulf of Mexico: 1. Distribution and air-sea CO_2 flux. *Journal of Geophysical Research: Oceans*, *120*, 1429–1445. https://doi.org/10.1002/2014JC010498

Jiang, L.-Q., Cai, W.-J., Wanninkhof, R., Wang, Y., & Lüger, H. (2008). Air-sea CO_2 fluxes on the U.S. South Atlantic Bight: Spatial and seasonal variability. *Journal of Geophysical Research*, *113*, C07019. https://doi.org/10.1029/2007JC004366

Laruelle, G. G., Cai, W.-J., Hu, X., Gruber, N., Mackenzie, F. T., & Regnier, P. (2018). Continental shelves as a variable but increasing global sink for atmospheric carbon dioxide. *Nature Communications*, *9*(1), 454. https://doi.org/10.1038/s41467-017-02738-z

Lee, K., Kim, T. W., Byrne, R. H., Millero, F. J., Feely, R. A., & Liu, Y. M. (2010). The universal ratio of boron to chlorinity for the North Pacific and North Atlantic oceans. *Geochimica et Cosmochimica Acta*, *74*(6), 1801–1811. https://doi.org/10.1016/j.gca.2009.12.027

Lohrenz, S. E., Cai, W.-J., Chakraborty, S., Huang, W.-J., Guo, X., He, R., et al. (2018). Satellite estimation of coastal pCO_2 and air-sea flux of carbon dioxide in the northern Gulf of Mexico. *Remote Sensing of Environment*, *207*, 71–83. https://doi.org/10.1016/j.rse.2017.12.039

Long, J., Hu, C., & Robbins, L. (2014). Whiting events in SW Florida coastal waters: A case study using MODIS medium-resolution data. *Remote Sensing Letters*, *5*(6), 539–547. https://doi.org/10.1080/2150704x.2014.933275

Long, J. S., Hu, C., Robbins, L. L., Byrne, R. H., Paul, J. H., & Wolny, J. L. (2017). Optical and biochemical properties of a Southwest Florida whiting event. *Estuarine, Coastal and Shelf Science*, *196*, 258–268. https://doi.org/10.1016/j.ecss.2017.07.017

Millero, F. J. (2010). Carbonate constants for estuarine waters. *Marine and Freshwater Research*, *61*(2), 139–142. https://doi.org/10.1071/MF09254

Park, G.-H., & Wanninkhof, R. (2012). A large increase of the CO_2 sink in the western tropical North Atlantic from 2002 to 2009. *Journal of Geophysical Research*, *117*, C08029. https://doi.org/10.1029/2011JC007803

Peters, W., Jacobson, A. R., Sweeney, C., Andrews, A. E., Conway, T. J., Masarie, K., et al. (2007). An atmospheric perspective on North American carbon dioxide exchange: CarbonTracker. *Proceedings of the National Academy of Sciences of the United States of America*, *104*, 18,925–18,930. https://doi.org/10.1073/pnas.0708986104

Raabe, E., Stonehouse, D., Ebersol, K., Holland, K., & Robbins, L. (2011). Detection of coastal and submarine discharge on the Florida Gulf Coast with an airborne thermal-infrared mapping system. *Professional Geologist*, *48*, 42–49.

Read, J. F. (1985). Carbonate platform facies models. *American Association of Petroleum Geologists Bulletin*, *69*(1), 860–878. https://doi.org/10.1306/ad461b79-16f7-11d7-8645000102c1865d

Reimer, J. J., Wang, H., Vargas, R., & Cai, W.-J. (2017). Multidecadal fCO_2 increase along the United States southeast coastal margin. *Journal of Geophysical Research: Oceans*, *122*, 10,061–10,072. https://doi.org/10.1002/2017JC013170

Robbins, L. L., Coble, P., Clayton, T. D., & Cai, W. -J. (2009). Ocean carbon and biogeochemistry scoping workshop on terrestrial and coastal carbon fluxes in the Gulf of Mexico, St. Petersburg, FL. (Open File Rep. 2009–1070, p. 46). Reston, VA: US Geological Survey.

Robbins, L. L., Hansen, M. E., Kleypas, J. A., & Meylan, S. C. (2010). CO2calc: A user-friendly seawater carbon calculator for Windows, Mac OS X, and iOS (iPhone). (Open File Rep. 2010–1280). Reston, VA: US Geological Survey.

Robbins, L. L., & Lisle, J. T. (2017). Regional acidification trends in Florida shellfish estuaries: A 20+ year look at pH, oxygen, temperature, and salinity. *Estuaries and Coasts*, 1–14. https://doi.org/10.1007/s1223

Robbins, L. L., Wanninkhof, L., Barbero, R., Hu, X., Mitra, S., Yvon-Lewis, S., et al. (2014). Air-sea exchange. In H. M. Benway & P. G. Coble (Eds.), *Ocean Carbon and Biogeochemistry Program and North American Carbon Program*, *Report of the U.S. Gulf of Mexico Carbon Cycle Synthesis Workshop* (pp. 17–23). Washington, DC: American Carbon Program.

Santos, I. R. S., Burnett, W. C., Chanton, J., Mwashote, B., Suryaputra, I. G. N. A., & Dittmar, T. (2008). Nutrient biogeochemistry in a Gulf of Mexico subterranean estuary and groundwater-derived fluxes to the coastal ocean. *Limnology and Oceanography*, *53*(2), 705–718. https://doi.org/10.4319/lo.2008.53.2.0705

Schijf, J., & Byrne, R. H. (2007). Progressive dolomitization of Florida limestone recorded by alkaline earth element concentrations in saline, geothermal, submarine springs. *Journal of Geophysical Research*, *112*, C01003. https://doi.org/10.1029/2006JC003659

Schlitzer, R. (2017). Ocean Data View. Retrieved from odv.awi.de

Smith, C. G., & Robbins, L. L. (2012). Surface-water radon-222 distribution along the West-Central Florida Shelf. (U.S. Geol. Surv. Open File Rep. 2012–1212, pp. 22). Reston, VA: U.S. Geological Survey.

Smith, C. G., & Swarzenski, P. W. (2012). An investigation of submarine groundwater—Borne nutrient fluxes to the West Florida Shelf and recurrent harmful algal blooms. *Limnology and Oceanography*, *57*(2), 471–485. https://doi.org/10.4319/lo.2012.57.2.0471

Sweeney, C., Karion, A., Wolter, S., Newberger, T., Guenther, D., Higgs, J. A., et al. (2015). Seasonal climatology of CO_2 across North America from aircraft measurements in the NOAA/ESRL global greenhouse gas reference network. *Journal of Geophysical Research: Atmospheres*, *120*, 5155–5190. https://doi.org/10.1002/2014JD022591

Troupin, C., Barth, A., Sirjacobs, D., Ouberdous, M., Brankart, J.-M., Brasseur, P., et al. (2012). Generation of analysis and consistent error fields using the Data Interpolating Variational Analysis (DIVA). *Ocean Modelling*, *52*(2012), 90–101. https://doi.org/10.1016/j.ocemod. 605 2012.05.002

Turner, R. E., Rabalais, N. N., & Justic, D. (2006). Predicting summer hypoxia in the northern Gulf of Mexico: Riverine N, P, and Si loading. *Marine Pollution Bulletin*, *52*(2), 139–148. https://doi.org/10.1016/j.marpolbul.2005.08.012

Wang, H., Hu, X., Cai, W.-J., & Sterba-Boatwright, B. (2017). Decadal fCO_2 trends in global ocean margins and adjacent boundary current-influenced areas. *Geophysical Research Letters*, *44*, 8962–8970. https://doi.org/10.1002/2017GL074724

Wang, Z. A., Wanninkhof, R., Cai, W.-J., Byrne, R. H., Hu, X., Peng, T. H., & Huang, W. J. (2013). The marine inorganic carbon system along the Gulf of Mexico and Atlantic coasts of the United States: Insights from a transregional coastal carbon study. *Limnology and Oceanography*, *58*(1), 325–342. https://doi.org/10.4319/lo.2013.58.1.0325

Wanninkhof, R. (2014). Relationship between wind speed and gas exchange over the ocean revisited. *Limnology and Oceanography: Methods*, *12*(6), 351–362. https://doi.org/10.4319/lom.2014.12.351

Wanninkhof, R., Barbero, L., Byrne, R., Cai, W. J., Huang, W. J., Zhang, J. Z., et al. (2015). Ocean acidification along the Gulf coast and East Coast of the USA. *Continental Shelf Research*, *98*, 54–71. https://doi.org/10.1016/j.csr.2015.02.008

Weiss, R. F. (1974). Carbon dioxide in water and seawater: The solubility of a non-ideal gas. *Marine Chemistry*, *2*(3), 203–215. https://doi.org/10.1016/0304-4203(74)90015-2

Wilson, J. L. (1975). *Carbonate Facies in Geologic History*. New York: Springer. https://doi.org/10.1007/978-1-4612-6383-8

Xue, Z., He, R., Fennel, K., Cai, W. -J., Lohrenz, S., & Hopkinson, C. (2013). Modeling ocean circulation and biogeochemical variability in the Gulf of Mexico. *Biogeosciences*, *10*(11), 7219–7234. https://doi.org/10.5194/bg-10-7219-2013

Xue, Z., He, R., Fennel, K., Cai, W. -J., Lohrenz, S., Huang, W. J., et al. (2016). Modeling pCO_2 variability in the Gulf of Mexico. *Biogeosciences*, *13*(15), 4359–4377. https://doi.org/10.5194/bg-13-4359-2016

Yao, W., & Byrne, R. H. (1998). Simplified seawater alkalinity analysis: Use of linear array spectrometers. *Deep Sea Research Part I Oceanographic Research Papers*, *45*(8), 1383–1392. https://doi.org/10.1016/S0967-0637(98)00018-1